SCIENTIFIC REPORTS

OPEN

Novel synthesis of topological insulator based nanostructures (Bi₂Te₃) demonstrating high performance photodetection

Alka Sharma[1,2], T. D. Senguttuvan[1,2], V. N. Ojha[1,2] & Sudhir Husale[1,2]

The rapid progress in 2D material research has triggered the growth of various quantum nanostructures- nanosheets, nanowires, nanoribbons, nanocrystals and the exotic nature originating through 2D heterostructures has extended the synthesis of hybrid materials beyond the conventional approaches. Here we introduce simple, one step confined thin melting approach to form nanostructures of TI (topological insulator) materials, their hybrid heterostructures with other novel 2D materials and their scalable growth. The substrate and temperature dependent growth is investigated on insulating, superconducting, metallic, semiconducting and ferromagnetic materials. The temperature dependent synthesis enables the growth of single, few quintuples to nanosheets and nanocrystals. The density of nanostructure growth is seen more on fabricated patterns or textured substrates. The fabricated nanostructure based devices show the broadband photodetection from ultraviolet to near infrared and exhibit high photoresponsivity. Ultimately, this unique synthesis process will give easy access to fabricate devices on user friendly substrates, study nanostructures and scalable growth will enable their future technology applications.

At nanoscale region, nanostructures compared to their bulk counterpart show quantum confinement effects resulting in exotic physical, and electronic transport properties. The growth of quantum nanostructure is highly desirable if the method is cost effective, capable of achieving scalable synthesis, growth on device friendly substrates and also applicable to form the heterostructures of novel materials. Since last few years, many 2D layered materials such as graphene, MoS_2, WS_2, BN, Bi_2Se_3, Bi_2Te_3 etc. have demonstrated exotic properties and showed their potential nanodevice applications. Among these the topological insulator, a new exotic state of matter, shows robust metallic surface states protected by time reversal symmetry which has attracted an immense interest in synthesis of these quantum nanostructures due to their potential applications in spintronics[1,2], thermoelectrics[3], dissipationless electronics[4], hosting Majorana fermions for quantum computation studies[5], broadband photovoltaic[6], infrared detectors[7], photodetectors[8–10] etc. The transport through topological surface states are often hindered due to the contribution coming from bulk of the material but quantum materials in 2D or 1D effectively enhance the surface transport suppressing the bulk contributions. The growth of these nanostructures can be achieved by using techniques such as molecular beam epitaxy (MBE)[11,12], vapor liquid solid (VLS)[13,14] or CVD[6], vapor solid (VS)[15,16], metal-organic chemical vapor deposition (MOCVD)[17,18], pulsed laser deposition (PLD)[19,20] and solvothermal methods[21,22] but most of such techniques are either expensive, need lattice matching, precursor molecules, chemicals, face great difficulty to form heterostructures and more importantly substrate used for deposition are not device friendly. Exfoliation[23,24] (mechanical or hydrothermal) is another simple approach but yield is often less and depositions of definite shapes of nano structures such as single quintuples, hexagons, nanowires are almost impossible.

Moreover the heterostructures of these novel materials when combined with other 2D materials give birth to many interesting puzzles and phenomena. Hence there is a great demand to synthesize a material from two or more materials aiming exciting desired properties and functionalities. But synthesis of such hybrid nanostructures

[1]Academy of Scientific and Innovative Research (AcSIR), National Physical Laboratory, Council of Scientific and Industrial Research, Dr. K. S Krishnan Road, New Delhi, 110012, India. [2]National Physical Laboratory, Council of Scientific and Industrial Research, Dr. K. S Krishnan Road, New Delhi, 110012, India. Correspondence and requests for materials should be addressed to S.H. (email: husalesc@nplindia.org)
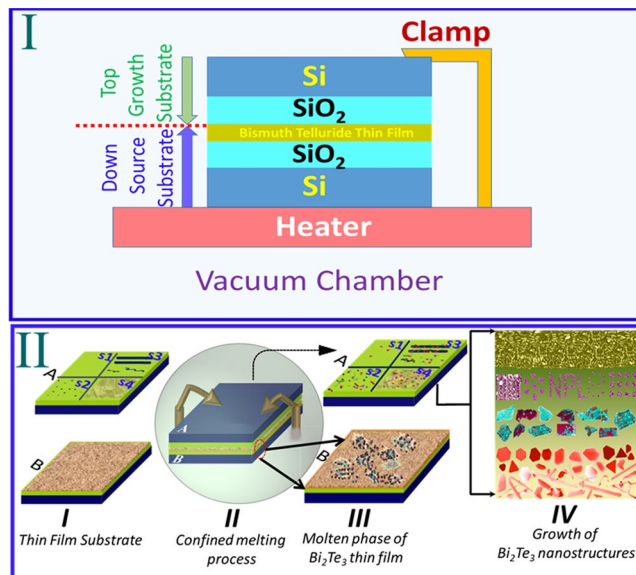
Figure 1. Schematic of the confined thin film melting method (cross sectional view I) and different steps (II). (II A) indicates the different types of substrate used for the growth of Bi₂Te₃ nanostructures. (B) shows the thin film deposited substrate.

is a complicated process for the present synthesis techniques. There is no general and simple solution for the fabrication of heterostructures and one step solution is needed for many applications that include photodetectors, biosensors, thermoelectric devices, solar cell, field effect transistors etc. Here we report simple catalyst, precursor, liquid free method which can synthesize these quantum nanostructures, their hybrid forms with high yield and offer a scalable approach on a device friendly substrate. Scalable manufacturing of van der Waals heterostructures might be possible with this method similar to vapor solid method which allows direct growth of topological insulator based nanostructures on 2D layered materials. This is a unique method compared to other techniques (Supplementary Information Table 1) and can be employed for synthesizing of other topological insulator based nanostructures and heterostructures with novel 2D materials.

Results and Discussion

Figure 1 shows the experimental schematics of confined thin film melting and substrate dependent growth of various nanostructures. Sections (I and II) represent the cross sectional view and simple steps of this method. Section (II A) represents the morphologically different types of substrates (s1–s4) used in this study and B is the sputter coated thin film. The confined melting process shows the top (growth) substrate (A) is in contact with the down (source) substrate (B) where sputtered deposited thin film of topological insulator (Bi₂Te₃) was mounted on a temperature controlled heater. The assembly was kept in vacuum chamber at pressure 10^{-5} mbar or better. After heating for >30 min the substrate assembly was cooled down to room temp. The molten species of Bi and Te were formed and simultaneously diffused on top substrate where these species get adsorbed and nucleate to form the nanosheets as shown in the figure. The substrates were detached at room temp and were used as it is for FESEM characterization. The growth of nanostructures, their shapes, sizes and density were found dependent on the heating temp and type of the substrate used for the growth (part-IV) which we have experimentally studied here.

Growth on device friendly substrates. The FESEM images shown in Fig. 2(a–h) represent the growth of Bi₂Te₃ nanostructures on insulating substrates silicon oxides and nitrides. Similar growth on other insulating substrate such as glass, quartz, sapphire are shown in Supplementary Information Fig. S1. Various thin nanowire or nanoribbon type of structures are visible in Fig. 2(a). The as grown nanosheets having shapes like hexagon, triangles are shown in Fig. 2(b,c). Growth of single (light contrast) and few quintuples (bright contrast) of Bi₂Te₃ are shown in Fig. 2(d). The thickness of the thinnest nanosheet was determined using AFM which is shown in the inset (Figure d) and the step height of ~1 nm indicates the single quintuple layer. Individual small dots, probably the nucleation points, were routinely observed at many places at the center of the single or few quintuple layers (Supplementary Information Fig. S2). Such nucleation center was also observed previously during the deposition of Sb₂Te₃ quintuples by vapor solid method[25]. The energy dispersive X ray (EDS) analysis is shown in the insets of the Fig. 2(e) which shows the presence of bismuth and tellurium elements with atomic compositions of about ~24.7 and 33.8%, respectively. The elemental mapping confirms the uniform distribution of these elements. The nanosheets, nanowire or nanoribbon type of structures grown on silicon nitride substrates are clearly visible in Fig. 2(f–h). The nanosheets were randomly distributed on these substrates. The lateral sizes of the nanosheets were observed from few hundreds of nanometer to microns and thickness was estimated using AFM (inset Fig. 2f). Many places we observed hexagonal, triangular morphologies with top flat surface indicating high quality growth which is important for device fabrication and quantum phenomena based basic studies. The high
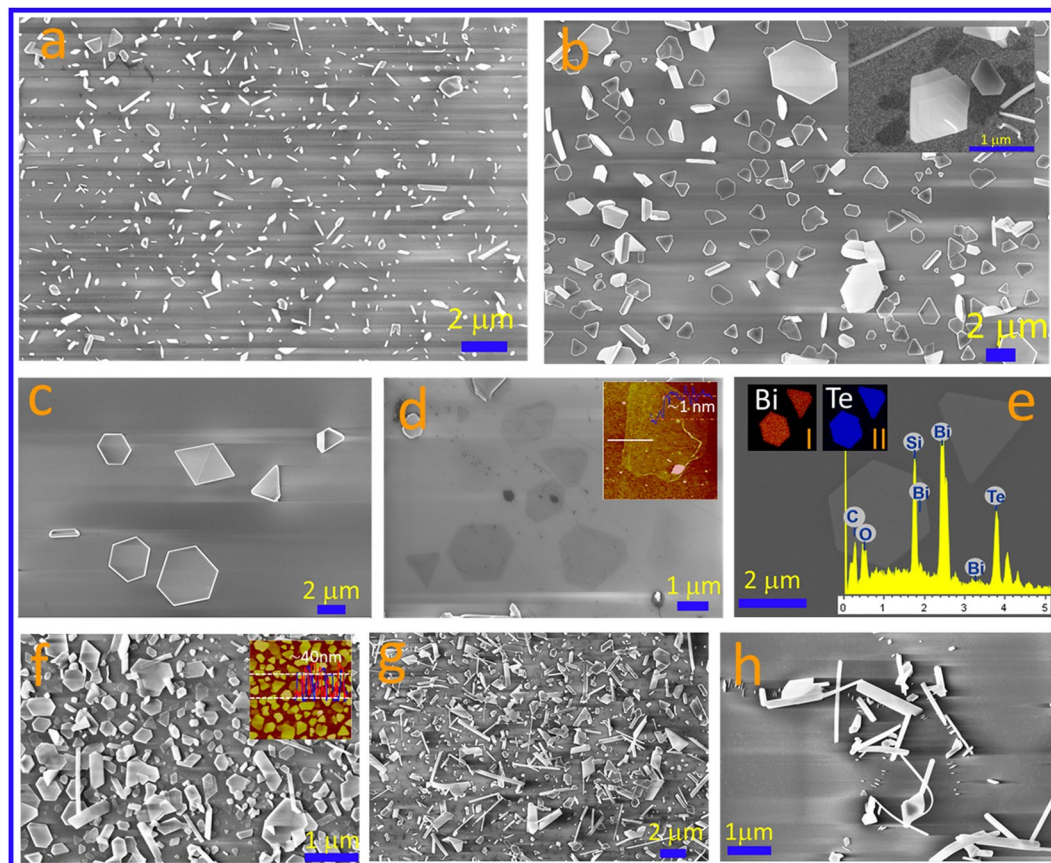
Figure 2. Growth on device friendly substrates (SiO$_2$ and Si$_3$N$_4$). (**a–h**) FESEM images representing (**a**) short nanowire and nanosheet like structures, (**b,c**) nanosheet dominated growth, inset (**b**) indicates the growth of different layers. Very thin nanosheets are visible in (**d**), AFM image (inset) estimates the growth of single quintuple. (**e**) Shows the EDS analysis of nanosheets. (**f–h**) Nanostructure growth on silicon nitride substrate, inset (**f**) shows the height measurement using AFM image.

crystalline quality of the material was observed and characterized by using HRTEM and Raman techniques which are shown in Supplementary Information Figs S3 and S4 respectively.

Growth on 2D layered materials. The coherent stacking of two different novel 2D materials forms the new exciting electronic system with unusual properties, phenomena and unique functionalities[26–28]. But the synthesis of TI nanostructures and their heterostructures with novel 2D materials is rare due to the complexity in the preparation of such quantum materials. Growth of Bi$_2$Te$_3$ nanostructures forming heterostructures with other 2D layered materials such as graphene, MoS$_2$ and Bi$_2$Se$_3$ is shown in Fig. 3. Micromechanically exfoliated flakes of 2D layered materials were deposited on SiO$_2$/Si substrate and same were used as to form the heterostructures. Figure 3(a) and its inset represent Frank –van der Merwe type growth of Bi$_2$Te$_3$ hexagonal nanosheets on graphene flakes. Growth shows random coverage with higher affinity towards the edges. At some places, these deposited nanosheets further act like seeds for the vertical growth of Bi$_2$Te$_3$ nanosheets (Stranski – Krastanov) as shown in Fig. 3(b). When thin film was melted at temp $\geq$ T$_m$ (melting temp of Bi$_2$Te$_3$), we find 3D type growth of nanocrystals (Volmer –Weber growth) indicating the less nucleation density and rapid growth as shown in Fig. 3(c). Here melting at high temp might provide the rapid interaction of adatoms with initial adsorbed molecule on the substrate. The flower type of growth was observed on Bi$_2$Se$_3$ nanosheets (Fig. 3d) whereas shapes like triangles or hexagons were distinguishable on the SiO$_2$ substrate as shown by the arrows in Fig. 3d. Note that bismuth selenide is also a low temp melting material and any distortion formed in lattice during heating may affect the nucleation and diffusive growth process. And here, we have observed the growth of large sheets without sharp edges covering most of the substrate flake area. The growth of Bi$_2$Te$_3$ nanostructures on MoS$_2$ is shown in Fig. 3(e–h). Similar to graphene substrate, growth of hexagons (Fig. 3e) at temp $<$ T$_m$ and nanocrystals (Fig. 3f) at temp $\geq$ T$_m$ were observed. The edges showed high coverage growth and vertical growth was also found reproducible. The growth of very tiny nanostructures was also noticed on few flakes (Fig. 3g,h).

Scalable growth on ITO substrate. Above results indicate that the growth of nanostructures is not uniform on flat insulating and 2D layered material substrates. Growth of quantum nanostructures on large area with high density and high reproducibility could be the key for many quantum technologies in future. The ITO coated glass shows very nice textured film with nano sized grain domains and boundaries as visible in Fig. 3(i)
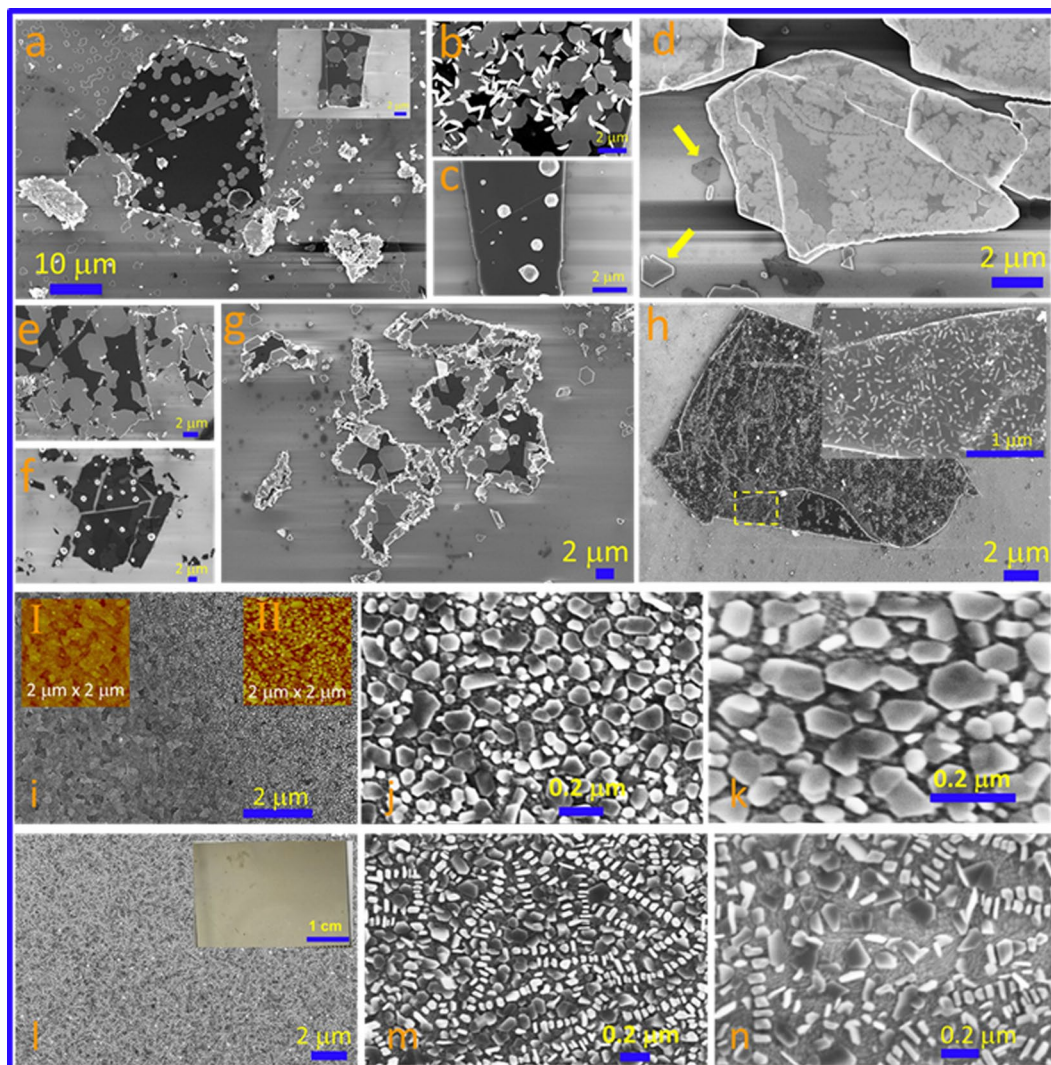
Figure 3. Heterostructure and scalable growth. (**a**–**h**) FESEM images demonstrating growth of Bi_2Te_3 nanostructures on graphene (**a**–**c**), Bi_2Se_3 (**d**) and MoS_2 flakes (**e**–**h**). (**i**–**n**) large area growth of Bi_2Te_3 nanostructures on ITO coated glass substrate. Inset I&II (**i**) represent the AFM image of ITO substrate and Bi_2Te_3 nanostructures on ITO substrate respectively. Inset (Figure l) represents the optical image demonstrating the possibility of scalable growth.

and inset of I shows AFM topographic image for the same. The growth area is clearly visible as compared to bare ITO substrate in Fig. 3(i). Insets of I and II represent AFM images of the bare ITO substrate and Bi_2Te_3 nanosheets grown on these substrates, respectively. Roughness of the textured film was around ~5 nm and the thickness of the nanosheets was estimated about ~15 nm from the AFM images. Figure 3(j,k) show the substrate triggered, high density growth of various Bi_2Te_3 nanosheets. Figure 3(l–n) show similar growth and densely packed nanosheets are clearly visible along with some vertically grown structures i.e. growth of the nanostructure perpendicular to the substrate. The lateral dimensions are less than micron size indicating the dangling bonds present on this substrate could restrict the lateral growth of the nanosheet and adatoms might prevent the lateral growth of the nanosheets and prefer vertical growth at some places. This indicates that the neighboring quintuples do not show van der Waals bonding. Important to note that the growth was observed over a large area, shown in the inset of Fig. 3(l), demonstrating scalability of this method which may find potential use in technological applications because of cost effectiveness and dense coverage over a large area.

Growth on lithographically patterned substrates. All the above results clearly show that substrate morphology play an important role in the growth of Bi_2Te_3 nanostructures. To study the density of the nanostructure growth and their affinity compared to flat substrate, we purposefully fabricated different types of patterns on insulating substrates and found interesting growth of Bi_2Te_3 nanostructures on these fabricated patterns. The growth of Bi_2Te_3 nanostructures on ebeam fabricated NiFe nanostrips is shown in Fig. 4(a–c). Since the edges give rise to high surface energy, more specific growth is expected on such patterns. Compared to substrate, high growth affinity on the nanostrips was clearly observed in Fig. 4(b–c). Insets (I &II) in Fig. 4(c) show elemental mapping of Bi and Te,
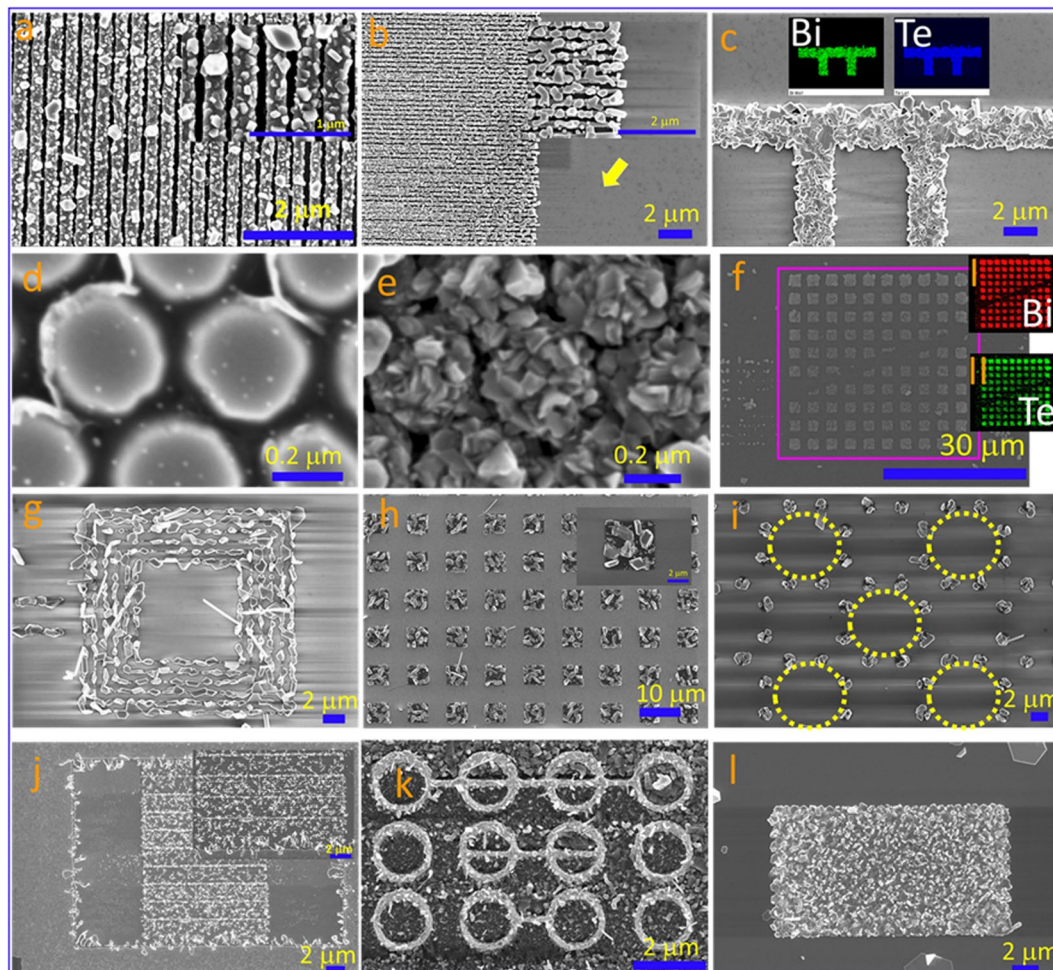
Figure 4. Growth of Bi_2Te_3 nanostructures on ebeam fabricated patterns (**a–i**) and FIB milled patterns (**j–l**). Inset I&II in Figure c and f show the elemental mapping obtained using EDS.

respectively, indicating the uniform distribution of the material. Topological quantum nanostructures integrated with superconducting material possess exciting exotic properties. Dots of Niobium were fabricated using ebeam lithography (Fig. 4d) and we found high density growth of Bi_2Te_3 nanostructures on these dots (Fig. 4e). High density growth was also observed on lithographically fabricated squares of Titanium (Ti) material (Fig. 4f) and insets I and II represent the elemental mapping of Bi and Te, respectively. More location specific systematic growth and arrangement of Bi_2Te_3 nanostructures were observed on fabricated patterns such as nested loops, arrays of squares, dots arranged in circular manner and they are shown in Fig. 4(g–i), respectively. Here similar to vapor solid growth, the presence of an impurity- dust, scratches, grains and grain boundaries, implanted ions etc. serves as a precursor and strongly helps during the growth of nanowires or nanosheets. We have observed that ion implantation i.e. pattern milled by FIB using Ga ion enhances the deposition of nanostructures (Fig. 4j–l). Note that the ion implantation also induces the additional compressive stress at localized area on the substrate and favors the atomic diffusion and growth of nanowires. Ion stress induced growth of nanowires on patterned area was studied earlier[29]. Single or less dense nanowires can be easily found with this method which is good for the device development research and the growth on patterned substrate is attractive and could be used as an alternative approach.

Temperature dependence on the growth of nanostructure. The Fig. 5(I) represents the temperature dependent evolution of different Bi_2Te_3 nanostructures observed in our study. The noticeable growth of nanowires, nanoribbons were routinely observed at temp ~350 °C (±50) along with very few thin nanosheets and the density of nanostructure growth was always dependent on the nucleation sites, defective and engineered places. Note that compared to Si/SiO$_2$/ITO substrates, bismuth telluride has a higher thermal expansion coefficient (TEC). Thus the sample heating impedes the expansion due to mismatch in TECs and induces the microscopic compressive stresses in Bi_2Te_3 film. The growth of Bi_2Te_3 nanowires due to the stress release or induced mass flow has been observed in sputtered deposited polycrystalline films[30] and thermal treatment used for the growth of CuO nanowires[31]. During heating, due to compressive stress, the mobile atoms e.g. Bi and Te preferably diffuse and accumulate at grain boundaries. Under cooling conditions, film undergoes tensile stress and diffused atoms move upward direction at the interface of Bi_2Te_3 thin film and may find an energetic nucleation sites for the growth of nanowires at the top substrate.
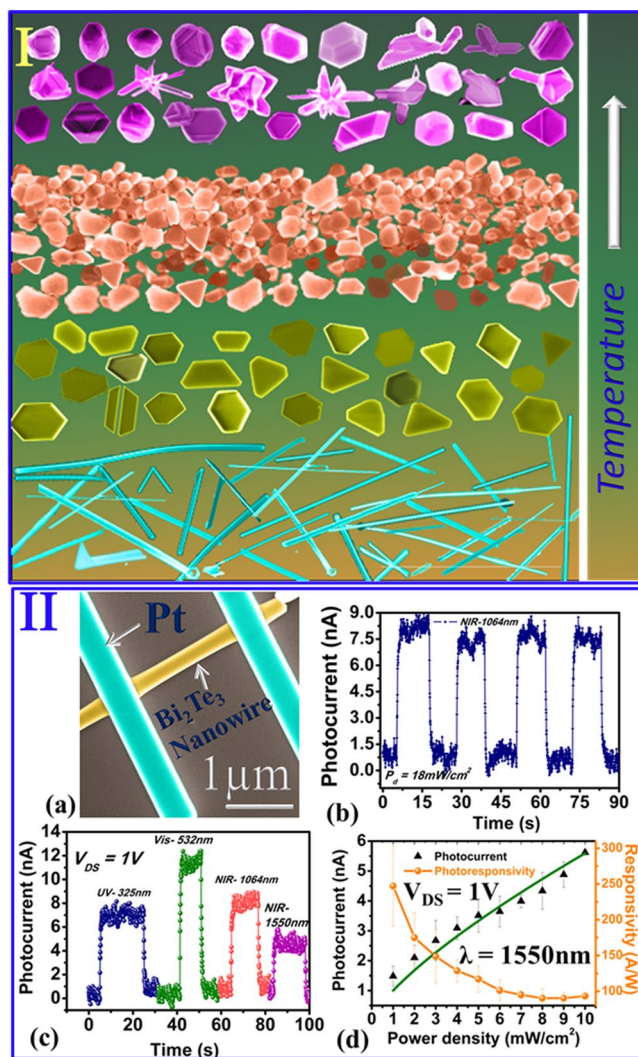
Figure 5. Temperature dependent growth of various Bi_2Te_3 nanostructures observed in this study and optoelectronic characterization of a Bi_2Te_3 nanowire device. (**a**) The false colour FESEM image of nanodevice. (**b**) The stability of nanowire device is examined under 1064 nm illumination. (**c**) Spectral dependent photocurrent–time domain of the nanowire at bias voltage 1 V. (**d**) The power density dependent photocurrent and responsivity of the Bi_2Te_3 nanowire device. The green curve shows the power law fitting of photocurrent at different power densities from 1 to 10 mW/cm².

For the temp range ~500 °C ($\pm$50), we mostly observed nanosheets of various shapes and sizes and very few nanowires or nanoribbons. The very high density of growth was noticed on textured (ITO coated glass) substrates at similar temperature. At this temperature, semi-molten phases could occur at many places in Bi_2Te_3 film which can be called as hot spots. During the cooling process probably a transformation in crystallization happens and tensile stress push might help for molecule adhesion, nucleation and subsequent growth at the top substrate. In case of ITO substrate, during cooling, molecules find many adhesion sites present on the textured ITO film where high density of growth was observed. During cooling/solidification, granular structure and grain boundaries act as substrates for the nucleation of the nanosheets by lowering the activation barrier and the closely spaced grains helps the simultaneous nucleations favored by low surface energy over a large surface. The growth and its dependence on the grains and grain boundaries present in the thin films are not investigated here. Ramping the temperature beyond ~650 °C ($\pm$50), we observed very consistent growth of thick nanocrystal like structures along with some few layered nanosheets on substrates like SiO_2, Si_3N_4, Graphene, MoS_2 or ITO.

Optoelectronics measurements. Further we have investigated the broadspectral photodetection properties of a Bi_2Te_3 nanowire grown by this method (Fig. 5(II)). Two probe optoelectrical measurements were carried out using Cascade Microtech instrument accompanied with Keithley 2634B source meter and light sources - UV-325 nm ($P_d = 1$ to 13 mW/cm²), Visible - 532 nm ($P_d = 32$ mW/cm²), NIR-1064 nm ($P_d = 1$ to 18 mW/cm²) and 1550 nm ($P_d = 1$ to 10 mW/cm²). The nanowire was biased at constant 1 V and sudden increase in the current was observed due to the light illuminations of different wavelengths. We have observed the photocurrent

dependency on the incident laser light illumination and the systematic increase in photocurrent with increase in laser power density was studied using the relation $I_{ph} = P^{\theta}$. The photoresponsivity of the Bi_2Te_3 nanowire was estimated using relation, $R = \frac{I_{ph}}{P_d \cdot A}$, where, R is the photoresponsivity, I_{ph} is the photocurrent, P_d is the power density and A is the active area of the Bi_2Te_3 nanowire device. The maximum photoresponsivity of about ~286 A/W is observed for the nanowire at 1550 nm, which shows high performance compared to the earlier reported photoresponsivity of the Bi_2Te_3 based photodetectors[32–36]. Further the estimated rise, decay time constants and detectivity were observed about 250 ms, 195 ms and 6.6×10^9 Jones, respectively.

Conclusion

In conclusion, we report synthesis of topological quantum materials and their hybrid forms on planar substrates like $SiN/SiO_2/ITO$ by a very simple cost effective technique eliminating the need of expensive instruments, precursors or catalyst. Compared to expensive or complicated methods, one step synthesis (assuming the availability of source and growth substrate) is simple and more attractive because the results show that the growth of bismuth telluride nanostructures (quintuples, nanosheets, nanoribbons and formation of heterostructures) can be achieved very easily on a device friendly substrate which makes this method more appealing for research in device fabrication and transport studies. The density of nanostructures and various shapes can be tuned using the substrate and the growth temperature, respectively. The data clearly shows the presence of Volmer–Weber (nanocrystals or thicker sheets), Frank–van der Merwe (2D nanosheet, layer by layer), and Stranski–Krastanov (single quintuple plus islands, mixed– layer and island) growths. This method can be universalized for other low melting temp based topological insulator materials and can form hybrid heterostructures with ease compared to other reported methods. High density nanosheet growth on textured film over a large area shows the scalability and the assembly of quantum nanostructures ready for future technological applications. Our experimental approach is simple but both the top and down substrates are in contact with each other, hence, for a clear understanding behind our results we need more theoretical and probably experimental designs in future. However the exotic nature of topological insulator based quantum nanostructures and their 2D hybrids may give new directions to synthesize the nanostructures and could find promising applications in nanoelectronics, optoelectronics, sensing, catalysis, energy storage and thermoelectrics.

Methods

Synthesis and electrical characterization of Bi_2Te_3 nanostructures. The substrates used in this study (silicon nitride, silicon oxide, quartz, sapphire, glass) were ultrasonicated in acetone and subsequently cleaned with acetone, isopropanol, methanol and DI water. Oxygen plasma treatment was performed prior to deposition of thin films and growth of nanostructures on these substrates. Source substrate (thin film of Bi_2Te_3) was made using sputtering technique and thickness of the film was optimized using AFM. After deposition of Bi_2Te_3 thin film, growth substrate was placed directly top on the sputtered thin film and was hold together using a gentle clamp. Heating was started once the vacuum of the chamber was in the range of about ~5×10^{-7} mbar or better. After heating substrates were cooled down to room temp and growth substrate was characterized using FESEM and optical microscopy. For device fabrication, big metal contact electrodes of Au~80 nm and Ti~10 nm were deposited on the growth substrate using shadow mask. Pt electrodes were directly deposited on the Bi_2Te_3 nanostructures using gas injection system (FIB attachment) and connected to big metal pads with the same technique. Electrical measurements were carried out in the probe station using source meter 2634B and laser light sources.

Data Availability

All experimental data required to evaluate and interpret the conclusions are present in the main manuscript or Supplementary Materials File.

References

1. Mellnik, A. R. *et al*. Spin-transfer torque generated by a topological insulator. *Nature* **511**, 449, https://doi.org/10.1038/nature13534 (2014).
2. Wang, Y. *et al*. Room temperature magnetization switching in topological insulator-ferromagnet heterostructures by spin-orbit torques. *Nat. Comm.* **8**, 1364, https://doi.org/10.1038/s41467-017-01583-4 (2017).
3. Xu, N., Xu, Y. & Zhu, J. Topological insulators for thermoelectrics. *npj Quant. Mater.* **2**, 51, https://doi.org/10.1038/s41535-017-0054-3 (2017).
4. Ogawa, N. *et al*. Zero-bias photocurrent in ferromagnetic topological insulator. *Nature Comm.* **7**, 12246, https://doi.org/10.1038/ncomms12246 (2016).
5. Jauregui, L. A., Pettes, M. T., Rokhinson, L. P., Shi, L. & Chen, Y. P. Magnetic field-induced helical mode and topological transitions in a topological insulator nanoribbon. *Nat. Nano.* **11**, 345, https://doi.org/10.1038/nnano.2015.293 (2016).
6. Wang, Z. H., Li, M. Z., Yang, L., Zhang, Z. D. & Gao, X. P. A. Broadband photovoltaic effect of n-type topological insulator Bi2Te3 films on p-type Si substrates. *Nano Res.* **10**, 1872–1879, https://doi.org/10.1007/s12274-016-1369-2 (2017).
7. Tang, W. W. *et al*. Ultrasensitive Room-Temperature Terahertz Direct Detection Based on a Bismuth Selenide Topological Insulator. *Adv. Fun. Mater.* **28**, https://doi.org/10.1002/adfm.201801786 (2018).
8. Sharma, A., Bhattacharyya, B., Srivastava, A. K., Senguttuvan, T. D. & Husale, S. High performance broadband photodetector using fabricated nanowires of bismuth selenide. *Sci. Rep.* **6**, https://doi.org/10.1038/srep19138 (2016).
9. Sharma, A., Srivastava, A., Senguttuvan, T. & Husale, S. Robust broad spectral photodetection (UV-NIR) and ultra high responsivity investigated in nanosheets and nanowires of Bi 2 Te 3 under harsh nano-milling conditions. *Sci. Rep.* **7**, 17911 (2017).
10. Wang, F. K. *et al*. Submillimeter 2D Bi2Se3 Flakes toward High-Performance Infrared Photodetection at Optical Communication Wavelength. *Adv. Fun. Mater.* **28**, https://doi.org/10.1002/adfm.201802707 (2018).
11. Chen, X., Ma, X. C., He, K., Jia, J. F. & Xue, Q. K. Molecular Beam Epitaxial Growth of Topological Insulators. *Adv. Mater.* **23**, 1162–1165, https://doi.org/10.1002/adma.201003855 (2011).
12. Li, Y. Y. *et al*. Intrinsic Topological Insulator Bi2Te3 Thin Films on Si and Their Thickness Limit. *Adv. Mater.* **22**, 4002–4007, https://doi.org/10.1002/adma.201000368 (2010).

13. Kong, D. S. *et al.* Topological Insulator Nanowires and Nanoribbons. *Nano Lett.* **10**, 329–333, https://doi.org/10.1021/nl903663a (2010).
14. Meister, S. *et al.* Synthesis and characterization of phase-change nanowires. *Nano Lett.* **6**, 1514–1517, https://doi.org/10.1021/nl061102b (2006).
15. Fang, L. *et al.* Catalyst-Free Growth of Millimeter-Long Topological Insulator Bi2Se3 Nanoribbons and the Observation of the pi-Berry Phase. *Nano Lett.* **12**, 6164–6169, https://doi.org/10.1021/nl302989v (2012).
16. Tu, N. H. *et al.* Large-Area and Transferred High-Quality Three-Dimensional Topological Insulator Bi2-xSbxTe3-ySey Ultrathin Film by Catalyst-Free Physical Vapor Deposition. *Nano Lett.* **17**, 2354–2360, https://doi.org/10.1021/acs.nanolett.6b05260 (2017).
17. Alegria, L. D. & Petta, J. R. Controlled MOCVD growth of Bi2Se3 topological insulator nanoribbons. *Nanotechnology* **23**, https://doi.org/10.1088/0957-4484/23/43/435601 (2012).
18. Cao, H. L. *et al.* Topological insulator Bi2Te3 films synthesized by metal organic chemical vapor deposition. *Appl. Phy. Lett.* **101**, https://doi.org/10.1063/1.4760226 (2012).
19. Yao, J. D. & Yang, G. W. Flexible and High-Performance All-2D Photodetector for Wearable Devices. *Small* **14**, https://doi.org/10.1002/smll.201704524 (2018).
20. Yao, J. D., Shao, J. M., Li, S. W., Bao, D. H. & Yang, G. W. Polarization dependent photocurrent in the Bi2Te3 topological insulator film for multifunctional photodetection. *Sci. Rep.* **5**, https://doi.org/10.1038/srep14184 (2015).
21. Wang, W. Z., Poudel, B., Yang, J., Wang, D. Z. & Ren, Z. F. High-yield synthesis of single-crystalline antimony telluride hexagonal nanoplates using a solvothermal approach. *J. Am. Chem. Soc.* **127**, 13792–13793, https://doi.org/10.1021/ja054861p (2005).
22. Zhu, H. T. *et al.* Tri-wing bismuth telluride nanoribbons with quasi-periodic rough surfaces. *J. Mater. Chem.* **21**, 12375–12380, https://doi.org/10.1039/c1jm11715g (2011).
23. Cho, S. J., Butch, N. P., Paglione, J. & Fuhrer, M. S. Insulating Behavior in Ultrathin Bismuth Selenide Field Effect Transistors. *Nano Lett.* **11**, 1925–1927, https://doi.org/10.1021/nl200017f (2011).
24. Ren, L. *et al.* Large-scale production of ultrathin topological insulator bismuth telluride nanosheets by a hydrothermal intercalation and exfoliation route. *J. Mater. Chem.* **22**, 4921–4926, https://doi.org/10.1039/c2jm15973b (2012).
25. Yang, F. *et al.* Scalable synthesis of two-dimensional antimony telluride nanoplates down to a single quintuple layer. *RSC Adv.* **5**, 59320–59325, https://doi.org/10.1039/c5ra03364k (2015).
26. Geim, A. K. & Grigorieva, I. V. Van der Waals heterostructures. *Nature* **499**, 419–425, https://doi.org/10.1038/nature12385 (2013).
27. Liu, Y. *et al.* Van der Waals heterostructures and devices. *Nat. Rev. Mater.* **1**, https://doi.org/10.1038/natrevmats.2016.42 (2016).
28. Novoselov, K. S., Mishchenko, A., Carvalho, A. & Neto, A. H. C. 2D materials and van der Waals heterostructures. *Science* **353**, https://doi.org/10.1126/science.aac9439 (2016).
29. Na, H., Eun, Y., Kim, M. O., Choi, J. & Kim, J. Low-Temperature Selective Growth of Tungsten Oxide Nanowires by Controlled Nanoscale Stress Induction. *Sci. Rep.* **5**, https://doi.org/10.1038/srep18265 (2015).
30. Ham, J. *et al.* Direct Growth of Compound Semiconductor Nanowires by On-Film Formation of Nanowires: Bismuth Telluride. *Nano Lett.* **9**, 2867–2872, https://doi.org/10.1021/nl9010518 (2009).
31. Jiang, X. C., Herricks, T. & Xia, Y. N. CuO nanowires can be synthesized by heating copper substrates in air. *Nano Lett.* **2**, 1333–1338, https://doi.org/10.1021/nl0257519 (2002).
32. Yao, J. D., Shao, J. M., Wang, Y. X., Zhao, Z. R. & Yang, G. W. Ultra-broadband and high response of the Bi2Te3-Si heterojunction and its application as a photodetector at room temperature in harsh working environments. *Nanoscale* **7**, 12535–12541, https://doi.org/10.1039/c5nr02953h (2015).
33. Yao, J. D., Zheng, Z. Q. & Yang, G. W. Layered-material WS2/topological insulator Bi2Te3 heterostructure photodetector with ultrahigh responsivity in the range from 370 to 1550 nm. *J. Mater. Chem. C* **4**, 7831–7840, https://doi.org/10.1039/c6tc01453d (2016).
34. Liu, J. J. *et al.* Bi$_2$Te$_3$ photoconductive detectors on Si. *App. Phy. Lett.* **110**, 141109, https://doi.org/10.1063/1.4979839 (2017).
35. Yao, J. D., Zheng, Z. Q. & Yang, G. W. All-Layered 2D Optoelectronics: A High-Performance UV-vis-NIR Broadband SnSe Photodetector with Bi2Te3 Topological Insulator Electrodes. *Adv. Fun. Mater.* **27**, https://doi.org/10.1002/adfm.201701823 (2017).
36. Qiao, H. *et al.* Broadband Photodetectors Based on Graphene-Bi2Te3 Heterostructure. *ACS Nano* **9**, 1886–1894, https://doi.org/10.1021/nn506920z (2015).

Acknowledgements

Author Contributions

A.S. performed the synthesis of nanostructures using sputtering system, carried out all the optoelectronic measurements, analysed HRTEM and Raman characterization data, schematics, figures and fabricated the nanodevices with S.H. T.D.S. and V.N.O. provided FIB tools, operational support and materials. S.H. conceived, designed the overall experimental strategy, supervised the research and wrote the manuscript. All the authors read and commented on the manuscript.

Additional Information

Supplementary information accompanies this paper at https://doi.org/10.1038/s41598-019-40394-z.

Competing Interests: The authors declare no competing interests.

Publisher's note: Springer Nature remains neutral with regard to jurisdictional claims in published maps and institutional affiliations.